Bioorganic & Medicinal Chemistry 20 (2012) 7175–7183

Contents lists available at SciVerse ScienceDirect

Bioorganic & Medicinal Chemistry

journal homepage: www.elsevier.com/locate/bmc

N-Phenyl-4-hydroxy-2-quinolone-3-carboxamides as selective inhibitors of mutant H1047R phosphoinositide-3-kinase (PI3Kα)

Dima A. Sabbah [a], Neka A. Simms [b], Wang Wang [b], Yuxiang Dong [a], Edward L. Ezell [c], Michael G. Brattain [b], Jonathan L. Vennerstrom [a], Haizhen A. Zhong [d,*]

[a] College of Pharmacy, University of Nebraska Medical Center, 986025 Nebraska Medical Center, Omaha, NE 68198-6025, USA
[b] Eppley Cancer Institute, University of Nebraska Medical Center, 985920 Nebraska Medical Center, Omaha, NE 68198-5950, USA
[c] Eppley Cancer Institute, University of Nebraska Medical Center, 986805 Nebraska Medical Center, Omaha, NE 68198-6805, USA
[d] Department of Chemistry, University of Nebraska at Omaha, DSC 362, 6001 Dodge Street, Omaha, NE 68182, USA

ARTICLE INFO

Article history:
Received 14 June 2012
Revised 18 September 2012
Accepted 25 September 2012
Available online 12 October 2012

Keywords:
PI3K
Selectivity
Colon cancer
AKT phosphorylation
Apoptosis

ABSTRACT

This work describes our efforts to optimize the lead PI3Kα inhibitor *N*-benzyl 4-hydroxy-2-quinolone-3-carboxamide using structure-based design and molecular docking. We identified a series of *N*-phenyl 4-hydroxy-2-quinolone-3-carboxamides as selective inhibitors of mutant H1047R versus wild-type PI3Kα and we also showed that the cell growth inhibition by these compounds likely occurs by inhibiting the formation of pAKT and induction of apoptosis.

1. Introduction

Phosphatidylinositol 3-kinases (PI3Ks) phosphorylate phosphatidylinositol 4,5-biphosphate (PIP_2) to generate 3,4,5-triphosphate (PIP_3), which phosphorylates downstream signaling proteins such as AKT, leading to increase cell growth and proliferation. PI3Ks are negatively regulated by the phosphatase and tensin homolog protein (PTEN), which dephosphorylates PIP_3.[1–3] PI3Ks are divided into three classes based on their substrate specificity and primary structures. Class IA comprises the PI3Kα, β, and δ isoforms encoded by their respective genes PIK3CA, PIK3CB, and PIK3CD.[4] PI3Kα mutations (E545K and E542K in the helical domain, and H1047R in the kinase domain) are observed in breast (27%), endometrial (24%), colon (15–32%), brain (27%), stomach, and upper digestive tract (19–25%) tumors.[5–7] The PI3Kα H1047R mutant has a 2-fold increase in lipid kinase activity, and thus poses a unique potential to decrease the efficacy of anticancer drugs targeting PI3Kα.[8] Thus, selective inhibition of PI3Kα mutants may provide additional therapeutic benefits. Numerous PI3Kα inhibitors have been reported[9–14] and some of these have progressed to clinical trials.[15–17] Yet few of these are PI3Kα mutant-selective.

By means of pharmacophore modeling and database searching, we identified *N*-benzyl 4-hydroxy-2-quinolone-3-carboxamide (**1**) as a lead compound with IC_{50} values of 1.1 and 0.73 μM against the wild-type (WT) PI3Kα and mutant (MUT) H1047R PI3Kα, respectively (Fig. 1).[18] Compound **1** suppressed the formation of pAKT and induced apoptosis in a human colon carcinoma cell line. We previously suggested that it might be possible to identify selective inhibitors of the H1047R mutant PI3Kα guided by the structural differences between the mutant and wild-type enzyme.[19] This work describes our efforts in optimizing **1**, which led to the discovery of a series of *N*-phenyl-4-hydroxy-2-quinolone-3-carboxamides with selectivity for the H1047R mutant PI3Kα.

2. Chemistry

Target compounds were designed to probe the contribution of the lactam and phenolic oxygen atoms (**2**–**4**), benzylic carbon (**5**), and the lactam hydrogen (**6**) to the activity of **1**. Compounds **2** and **4**[20–22] were prepared by HOBt/EDCl couplings of the corresponding quinoline-3-carboxylic acids with benzylamine. Herein we reported for the first time, ^1H and ^{13}C NMR spectra of **2** and **4**. Target compounds **5** and **7**–**11** were prepared in neat one-pot reactions (Scheme 1) between triethyl methanetricarboxylate (**12**) and the corresponding anilines (**13**) at 170–195 °C for 6 h. Target compound **6**[23,24] was prepared by methylation of **5**

* Corresponding author. Tel.: +1 402 554 3145; fax: +1 402 554 3888.
E-mail address: hzhong@unomaha.edu (H.A. Zhong).

0968-0896/$ - see front matter © 2012 Elsevier Ltd. All rights reserved.
http://dx.doi.org/10.1016/j.bmc.2012.09.059

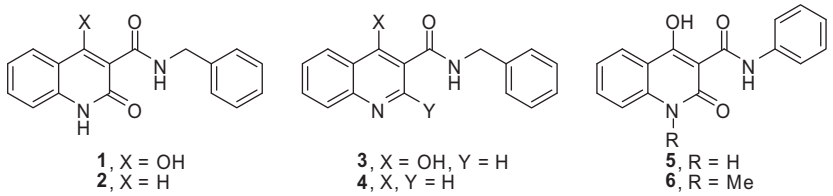

Figure 1. Analogues of lead compound (**1**).

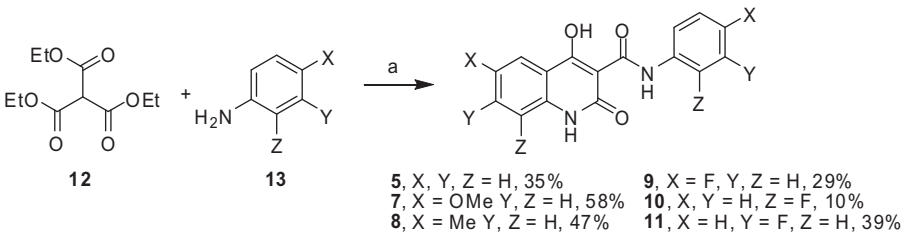

Scheme 1. Conditions: (a) 170–195 °C, 6 h.

(dimethyl sulfate/cesium carbonate/DMF). Target compound **3** was commercially available. Structural elucidation of the target compounds was determined by ^{1}H and ^{13}C NMR and elemental analysis; in some cases, they were further characterized by 2D NMR (HMBC, HSQC, and COSY) (Tables S1 and S2). Assigning the ^{13}C NMR chemical shifts of **9**–**11** was assisted by calculation and comparison of the chemical shifts to those of **5** and known fluorinated substituted benzenes.[20] Our 2D-NMR data also confirm that **1** (2-keto and 4-enol), **2** (2-keto), and **3** (4-enol) are the observed tautomers for these target compounds.

3. Results and discussion

The growth inhibition of the HCT116 colon cancer cell lines (both WT and H1047R MUT) by compounds **1**–**6** is shown in Table 1. HCT116 is a highly malignant colon carcinoma cell line harboring both wild-type and mutant (H1047R) PI3Kα, and it was produced from a primary tumor tissue culture.[25] The colon carcinoma cell lines containing only wild-type (WT) or mutant H1047R (MUT) PI3Kα were prepared by asymmetrical knockout of the MUT and WT genes, and are denoted as HCT116-WT and HCT116-MUT, respectively.[26]

The one to two-order of magnitude loss of potency for **2**–**4** versus **1** reveal that the lactam and the phenolic oxygen atoms of **1** are required for good PI3Kα inhibition (Table 1), an outcome supported by our docking experiments (Fig. 2). To investigate the binding mode of **1** to H1047R mutant and to investigate the necessity of both the lactam and the phenolic groups, we applied induced-fit docking[27] of **1** to the H1047R mutant model. The top ten docked poses from the induced-fit docking were clustered and classified as either mode A or mode B. Four out of 10 docked poses adopted mode A, and 5 out of 10 exhibited mode B (Fig. 2).

Table 1
Growth inhibition IC_{50} (μM) of the HCT116-WT and HCT116-MUT (H1047R) cell lines

Compounds	HCT116-WT	HCT116-MUT (H1047R)
LY294002[a]	6.7	5.3
1[a]	1.1	0.73
2	420	330
3	24	19
4	65	120
5	9.4	2.5
6	110	100

[a] IC_{50} data from Sabbah et al.[18]

The remaining docked pose adopted a conformation different from those observed in modes A and B. These docking results suggest that the lactam and the phenolic oxygen (4-OH) atoms form important H-bonds in the PI3Kα binding pocket; in binding mode A, the 4-OH and the amide carbonyl groups form two H-bonds with Glu849 and Val851, whereas in binding mode B, the lactam functional group forms H-bonds with the main chain NH and carbonyl groups of Val851. Compound **1**, with both lactam and the phenolic functional groups, maximizes the H-bond interactions with PI3K, and therefore binds more tightly than compounds **2**, **3**, and **4**, which have only one or none of these two essential functional groups. The growth inhibition data (Table 1) support the importance of these interactions. The significantly diminished inhibition of both the WT and MUT colon cancer cell lines by **6**, the *N*-methyl derivative of **5**, confirms the important contribution of the lactam NH to interaction with PI3Kα.

The data for **5** shows that the benzylic carbon atom of **1** plays a less important role in PI3Kα inhibition; although **5** is slightly less potent than **1**, it is similar to LY294002[18] in potency with some selectivity for inhibition of the HCT116-MUT (H1047R) cell line. Intrigued by this result, we envisioned that simple derivatives of **5** might have increased selectivity for inhibition of the HCT116-MUT (H1047R) cell line.

Glide docking studies of **5** and its derivatives **7**–**11** into WT (PDB id:2RD0)[4] and MUT (H1047R) PI3Kα (PDB id:3HHM)[28] were used to guide molecule design. These data showed that target compounds **7**–**11** show comparable docking scores to that of **5**, suggesting that they might have similar binding affinities to **5** (Table 2). Moreover, **1** and **5** match the same pharmacophoric points (Fig. 3), suggesting that although **5** does not have the methylene group of **1**, it occupies a similar binding pocket, in good agreement with what we observed experimentally (Table 1). The more negative docking scores for **5**, **7**, **9**–**11** toward the MUT PI3Kα isoform suggested that these compounds might be mutant-selective. These computational data suggest that **7**–**11** may have similar potencies yet better selectivities than those of the lead compound **1**. Figure S1 showed that the calculated docking scores (kcal/mol) are positively correlated with the experimentally obtained IC_{50}s, suggesting that docking scores could be used to predict ligand binding affinities.

Table 3 shows that compounds **5**, and **7**–**11** inhibit both WT and MUT (H1047R) PI3Kα isoforms. As measured by the selectivity index, they were generally more potent against the H1047R mutant with IC_{50s} in the same range of that of LY294002 (especially

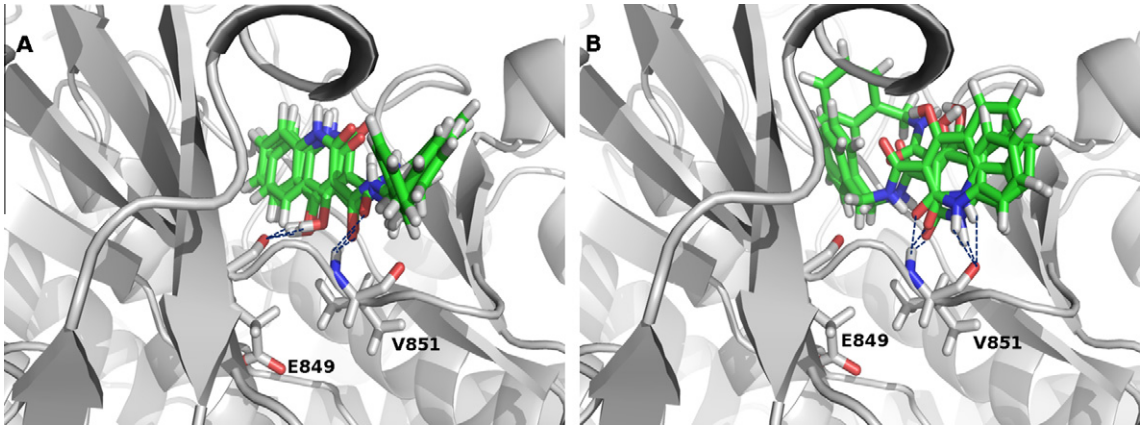

Figure 2. Two binding modes of **1** in the PI3Kα kinase catalytic site. (A) The first binding conformation: the C4 phenol and the amide carbonyl group bind to E849 and V851, respectively. (B) The second binding conformation: the C2 (CO and NH) of the lactam bind to V851. The C atoms of **1** are depicted in green; the H atoms in white; the O atoms in red; and the N atoms in blue.

Table 2
Glide docking scores (kcal/mol) against the WT and MUT PI3Kα

Compound	Docking score (Kcal/mol)	
	WT PI3Kα (2RD0)	MUT (H1047R) PI3Kα (3HHM)
1	−12.0	−10.4
5	−9.20	−9.97
7	−7.30	−9.68
8	−11.3	−10.6
9	−10.1	−10.9
10	−9.24	−10.3
11	−9.63	−10.6

Table 3
Growth inhibition (IC_{50}, μM) by *N*-phenyl-4-hydroxy-2-quinolone-3-carboxamides

Compounds	HCT116-WT	HCT116-MUT (H1047R)	Selectivity index (IC_{50} WT/IC_{50} MUT)
LY294002[a]	6.7	5.3	1.3
1[a]	1.1	0.73	1.5
5	9.4	2.5	3.8
7	64	6.3	10
8	27	5.6	4.8
9	15	6.9	2.2
10	22	3.6	6.0
11	6.5	0.28	23

[a] IC_{50} data from Sabbah et al.[18]

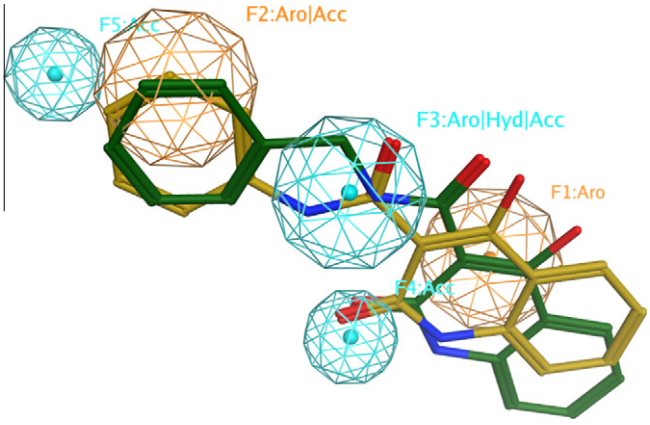

Figure 3. PI3Kα pharmacophore model with **1** (C atoms in green) and **5** (C atoms in yellow).

for the H1047R mutant-expressing cells), a reference compound used for PI3K inhibition studies. Of these, **7** and **11** showed the highest selectivities.

In order to determine whether growth inhibition of the colon cancer cell lines by **2**–**5** and **7**–**11** was mediated by the PI3K / AKT pathway, we performed PI3Kα kinase assays and immunoblot analyses of AKT activation in the HCT116-WT and HCT116-MUT cell lines. Compounds were tested at a single concentration that approximately corresponded to the range of the previously determined cell growth inhibition IC_{50} data (Tables 1 and 3). For instance, larger concentrations were used in the pAKT and apoptosis assays for compounds **2**, **4**, and **7** because of their higher IC_{50}s in growth inhibition assays.

For the HCT116-WT cell lines (both WT and MUT), all compounds inhibited PI3Kα with activities comparable to that of LY294002. Normalization of kinase inhibition effect (Fig. 4C and D, and Table 4) was performed with LY294002 as a reference.

The immunoblot assay of pAKT-S473 and total AKT (Fig. 5) showed that all compounds inhibited the formation of phosphorylated AKT at Ser473 (pAKT-S473) in the MUT cell lines compared to DMSO. However, when compared to the reference compound LY294002, which most potently inhibited pAKT-S473 formation in HCT116-WT cells, only **2** and **5** inhibited the formation of pAKT-S473 in both WT and MUT with activities comparable to those of LY294002. It is intriguing to observe that **7**–**11** showed much weaker or no inhibition of pAKT-S473 formation in the WT cells compared to that of LY294002. Compounds **7** and **8** showed similar inhibition on pAKT-S473 in the MUT cells, whereas compounds **9**–**11** had much weaker activities. However, **9**–**11** inhibited MUT cell growth (Table 3) comparable to that of LY294002. This suggests that growth inhibitory activities of **9**–**11** in both the HCT116 WT and MUT cells might be mediated through alternative pathways not involving AKT activation. Excluding **9**–**11**, the other compounds at the indicated concentrations inhibited the formation of pAKT-S473 in the MUT cell lines comparable to that of LY294002. Similar to LY294002, **5** inhibited pAKT-S473 formation in both WT and MUT cells. The inhibition of WT PI3Kα and the inhibition of formation of pAKT-S473 by **2** in the WT cells are surprising, because the IC_{50}s of cell growth inhibition (Table 1) of **2** were 420 and 330 μM. In addition, none of the compounds had any effect on the expression of total AKT protein in either the WT or MUT cells indicating that they would not be expected to interrupt the normal functions of AKT.

We also assessed whether growth inhibition of the colon cancer cells by these compounds were mediated by an apoptotic

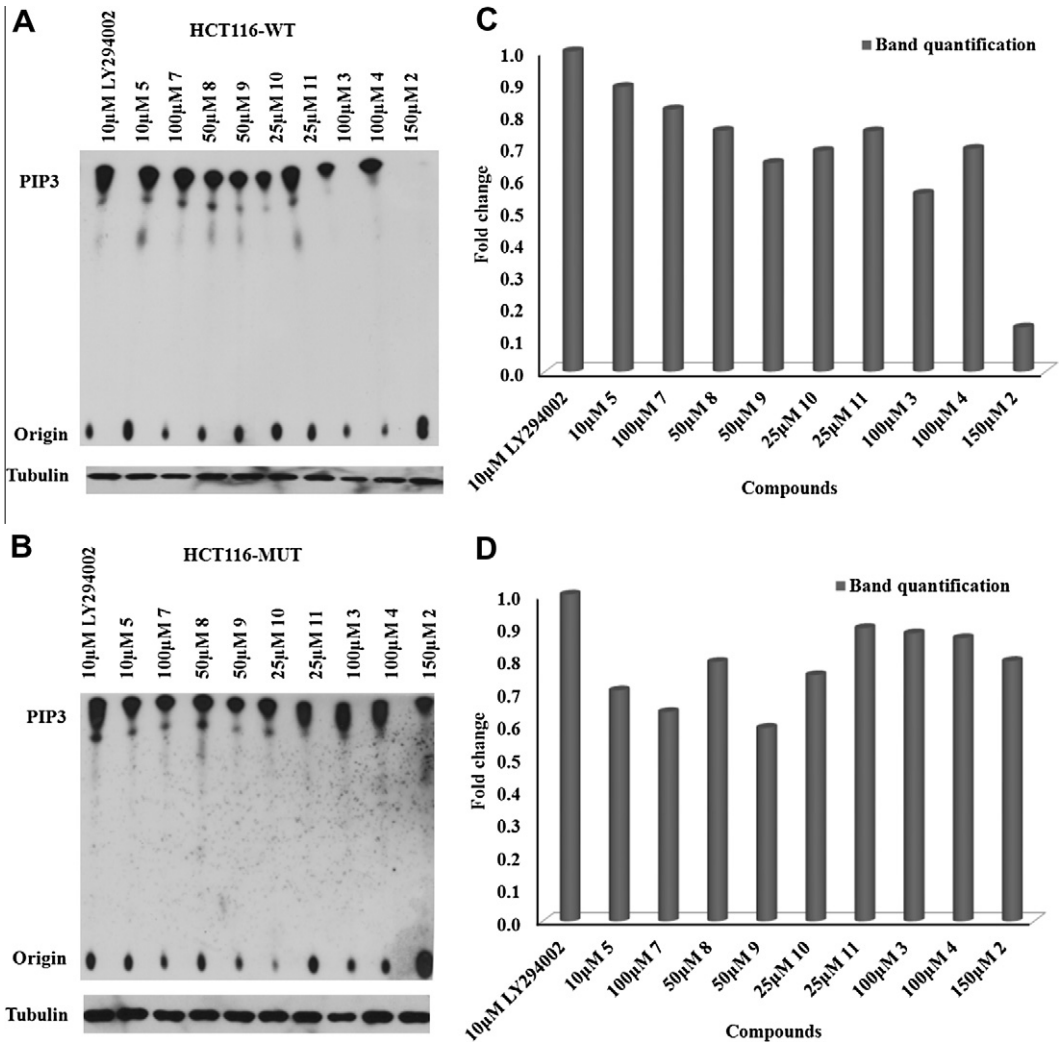

Figure 4. Direct inhibition of PI3K kinase activity by **2**–**5** and **7**–**11** in the WT (A) and H1047R MUT (B)1047R mutant (bottom). The areas of each band were calculated using Image J software and compared to LY294002 and the band quantification for kinase inhibition is labeled for the WT (C) and MUT (D).

Table 4
Normalized activities against PI3K kinase and the apoptosis (cleaved PARP) using LY294002 (1.0-fold) as a reference, and the normalized activities against pAKT-S473 using DMSO (1.0-fold) as a reference

.	PI3K Kinase		pAKT-S473		Cleaved PARP	
	HCT116-WT	HCT116-MUT	HCT116-WT	HCT116-MUT	HCT116-WT	HCT116-MUT
LY294002	1.00	1.00	0.01	0.41	1.00	1.00
5	0.89	0.71	0.11	0.40	0.01	4.99
7	0.82	0.64	1.66	0.44	0.01	3.90
8	0.75	0.79	1.66	0.41	1.00	1.14
9	0.65	0.59	0.95	0.86	1.01	1.37
10	0.69	0.75	1.60	1.23	0.88	5.05
11	0.75	0.90	1.01	0.51	0.40	1.35
3	0.56	0.88	1.00	0.20	0.71	0.20
4	0.70	0.87	1.59	0.30	0.81	0.06
2	0.14	0.80	0.09	0.13	0.92	0.05

Note: In PI3K kinase and pAKT-S473 assays, the smaller the number, the less PIP_3 that was generated, the more PI3Kα that was inhibited, and thus the less AKT that was phosphorylated. For the apoptosis assay, the larger the number, the more cleaved PARP that was generated, the more apoptosis that was induced.

mechanism by using a poly-(ADP-ribose) polymerase (PARP) cleavage detection assay in both HCT116-WT and MUT cells (Fig. 6). The appearance of cleaved products of PARP (88 kDa) is widely used as an indicator of apoptosis.[29,30] Assessing PARP cleavage in the HCT116-WT cells showed that, except for **5** and **7**, all compounds induced some apoptosis in the WT cell line. Interestingly, LY294002 (10 μM) induced little apoptosis in HCT116-MUT cells, whereas compounds **5**, **7**, and **10** were much more effective in inducing apoptosis. However, compounds **8**, **9** and **11** did not induce much apoptosis in the MUT cells (Fig. 6).

To quantify the activities of tested compounds, we used Image J software to calculate the areas of the bands in Figures 4–6 and

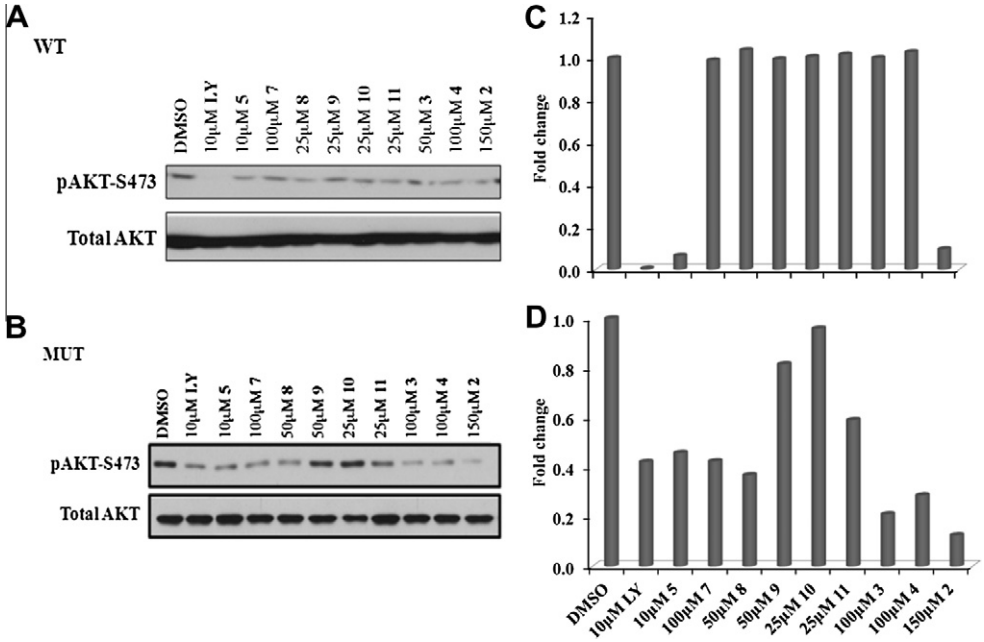

Figure 5. Inhibition of total AKT and phosphorylated AKT at Ser473 (pAKT-S473) by **2**–**5** and **7**–**11** in the WT (A) and the H1047R MUT (B) 1047R mutant (bottom). The areas of each band were calculated using Image J software and compared to LY294002 and the band quantification for pAKT formation is labeled for the WT (C) and MUT (D). The compounds in X-axis in C and D are the same.

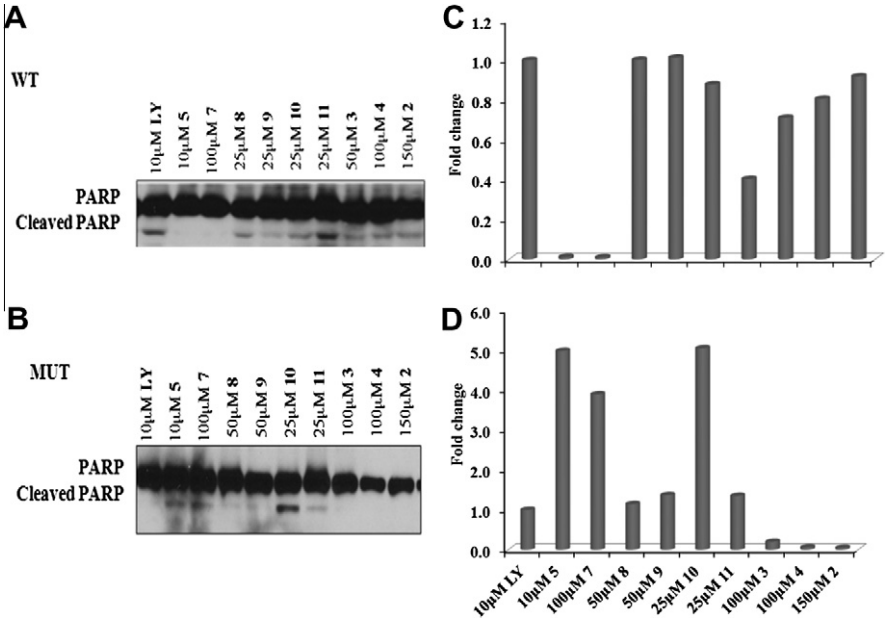

Figure 6. PARP cleavage by **2**–**5** and **7**–**11** in WT (top) and the H1047R MUT (bottom) 1047R mutant (bottom). The areas of each band were calculated using Image J software and compared to LY294002 and the band quantification for cleaved PARP formation is labeled for the WT (C) and MUT (D). The compounds in X-axis in C and D are the same.

quantified each band in comparison to LY294002 for the PI3K kinase and PARP cleavage tests, and DMSO for the AKT assay (Table 4). Table 4 showed that **5** inhibited PI3K kinase and formation of pAKT in both WT and MUT cells, but it induced apoptosis only in MUT cells. Table 4 also indicated that **7** and **10** induced more apoptosis in the MUT cells than LY294002. All three assays indicated that **7**–**11** were weaker inhibitors of PI3K kinase and pAKT formation than LY294002, suggesting that mechanisms other than the PI3K /AKT pathway may be involved to account for the observed apoptosis and/or growth inhibition.

In order to determine the structural basis for PI3Kα inhibition by these compounds, we employed induced fit docking (IFD) against the WT PI3Kα (2RD0) and MUT (H1047R) PI3Kα (3HHM).[26,27] The IFD approach was proposed by Sherman et al.[31,32] and has been successfully applied in our study of epidermal growth factor receptor (EGFR) inhibitors.[33] The IFD approach takes into consideration the conformational changes in proteins by the following method: ligands are docked to a protein in a rigid docking using softened-potential docking with the van der Waals radii for protein atoms at a 0.7 scaling using the Glide program[27,34,35] and the top ligand

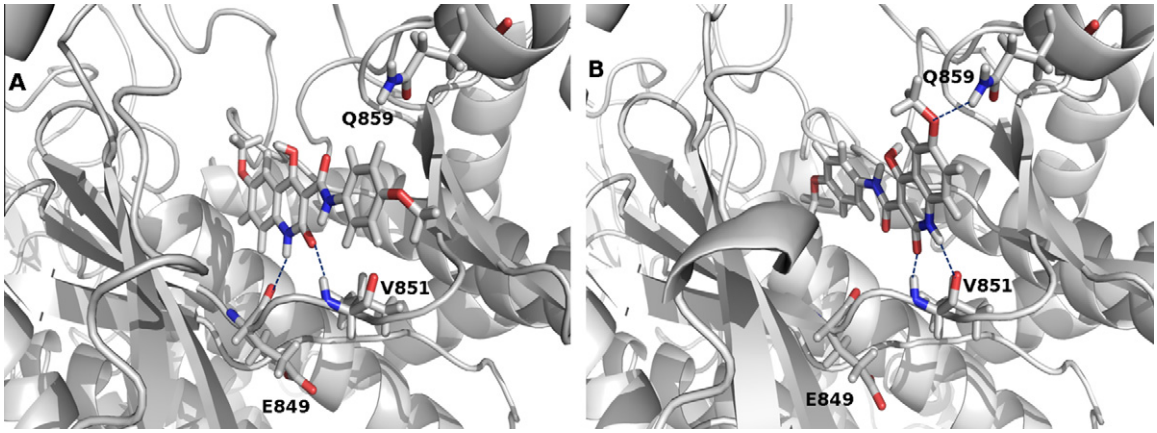

Figure 7. Binding conformations of **7** in (A) the wild-type PI3Kα (PDB ID:2RD0) and (B) mutant (H1047R) PI3Kα (PDB ID:3HHM) binding domains. H-bonds are depicted in dotted blue lines.

poses are then subjected to a minimization along with protein residues within 5 Å of ligands using the Prime program,[27] followed by a redocking procedure against the minimized protein. In this way, protein plasticity can be taken into account during the whole docking process.

Our IFD docking data for **1**, **5**, and **7**–**11** show that these compounds bind to the kinase cleft of both WT and MUT PI3Kα, particularly with the backbones of Tyr836, Glu849, Val851, Gln859, and Asp933. Other computational[19,36] and experimental[28] data also showed the significance of these key binding residues, especially Asp933. Our previous docking studies suggested the importance of Gln859 in designing mutant and/or isoform-specific PI3Kα inhibitors; the Gln859 in PI3Kα corresponds to Lys890 in PI3K γ.[19] Consistent with this hypothesis (Fig. 7), **7** has a 10-fold selectivity against MUT PI3Kα over WT PI3Kα and forms a H-bond with Gln859 of MUT H1047R. The induced-fit docking of **7** to the WT and MUT PI3Kα showed that **7** forms three H-bonds with Val851 and Gln859 of the MUT whereas it forms two H-bonds with Glu849 and Val851 in the WT.

4. Conclusions

Using both WT and H1047R MUT HCT116 colon cancer cell lines, this preliminary investigation of lead PI3Kα inhibitor **1** revealed that the lactam and the phenolic oxygen atoms are required for good PI3Kα inhibition, an outcome supported by docking experiments. We also discovered that *N*-phenyl-4-hydroxy-2-quinolone-3-carboxamides **5** and **7**–**11** were selective inhibitors of the MUT (H1047R) versus WT PI3Kα and also showed that the cell growth inhibition of **5** likely occurs by inhibiting the formation of pAKT and induction of apoptosis in MUT cells. The cell growth inhibition by **7**–**11**, however, is not mediated through the PI3K / AKT pathway. Whether differences in cellular bioavailability impact the activity differences between cell and enzyme assays remains to be determined. Induced fit docking (IFD) studies identified key residues that contribute to inhibitor binding to PI3Kα. Interestingly, **5**[23,24,37–39] was previously identified as an anti-angiogenic agent[24,40,41] and was investigated for the treatment of choroidal neovascularization.[39] In addition, compounds with the core structure of **5** decreased tumor volume, induced apoptosis, and generated hypoxia-induced death in human prostatic carcinoma cells[39] and had in vivo antitumor effects in rat and human prostate cancers[42–44] and in Lewis lung cell carcinoma cells.[45]

5. Experimental

5.1. Chemistry

1D-NMR spectra were recorded with a Varian INOVA 500 MHz spectrometer. Chemical shifts are expressed in δ units using the residual DMSO and $CDCl_3$ signals as the standard when measured in DMSO-d_6 and $CDCl_3$, respectively. 2D-NMR spectra were measured with Bruker Avance III 400-MHz spectrometer. Melting points were determined using Ez-melt apparatus. Elemental analyses were recorded on a PerkinElmer 2400 II series CHN analyzer and performed by M-H-W Labs, Phoenix, AZ.

5.1.1. *N*-Benzyl 2-hydroxyquinoline-3-carboxamide (2)

2-Hydroxyquinoline-3-carboxylic acid (95 mg, 0.5 mmol), benzylamine (64 mg, 0.6 mmol), 1-hydroxybenzotriazole (68 mg, 0.5 mmol), and triethylamine (152 mg, 1.5 mmol) were dissolved in dichloromethane (5 ml) and acetonitrile (10 ml). After the addition of 1-ethyl-3-(3-dimethylaminopropyl) carbodiimide hydrochloride (288 mg, 1.5 mmol), the mixture was stirred for 24 h at rt. The crude precipitate was filtered and washed by water, then by acetonitrile to give **2** as a white precipitate (94 mg, 68%); mp 248–250 °C; ^{1}H NMR (500 MHz, DMSO-d_6) δ 3.94 (s, 2H), 7.27–7.43 (m, 6H), 7.52 (d, J = 8.3 Hz, 1H), 7.61 (t, J = 7.8 Hz, 1H), 7.88 (d, J = 7.8 Hz, 1H), 8.64 (s, 1H); ^{13}C NMR (125.7 MHz, DMSO-d_6) δ 42.60, 118.01, 119.38, 120.73, 123.16, 128.22, 128.56, 128.63, 129.68, 132.50, 142.63, 143.56, 164.62, 166.22.

5.1.2. *N*-Benzyl quinoline-3-carboxamide (4)

3-Quinolinecarboxylic acid (87 mg, 0.5 mmol), benzylamine (64 mg, 0.6 mmol), 1-hydroxybenzotriazole (68 mg, 0.5 mmol), and triethylamine (152 mg, 1.5 mmol) were dissolved in acetonitrile (10 ml) for 5 min. After the addition of 1-ethyl-3-(3-dimethylaminopropyl) carbodiimide hydrochloride (288 mg, 1.5 mmol), the mixture was stirred for 24 h at rt. The acetonitrile was then evaporated and water was added. After filtration and drying, **4** was isolated as a white crystalline solid (192 mg, 73%); mp 141–143 °C; Lit. mp 139–144 °C[43–45]; ^{1}H NMR (500 MHz, $CDCl_3$) δ 4.72 (d, J = 5.9 Hz, 2H), 6.79 (s, 1H), 7.31–7.45 (m, 5H), 7.61 (t, J = 7.3 Hz, 1H), 7.78 (d, J = 7.3 Hz, 1H), 7.87 (t, J = 7.8 Hz, 1H), 8.13 (d, J = 8.8 Hz, 1H), 8.60 (d, J = 1.5 Hz, 1H), 9.27 (d, J = 2 Hz,1H); ^{13}C NMR (125.7 MHz, $CDCl_3$) δ 44.34, 126.86, 126.88, 127.55, 127.85, 128.04, 128.72, 128.90, 129.39, 131.30, 135.61, 137.76, 148.10, 149.28, 165.49.

5.1.3. *N*-Phenyl 4-hydroxy-2-quinolone-3-carboxamide (5)

Triethyl methanetricarboxylate (232 mg, 1 mmol) and aniline (93 mg, 1 mmol) were mixed and heated at 170–195 °C for six hours. The reaction was cooled to rt and treated with ethanol, filtered and washed with ethanol to give **5** as a yellow sandy compound (98 mg, 35%); mp 303–305 °C; Lit. Mp 298–305°C[32,34]; ^{1}H NMR (500 MHz, DMSO-d_6) δ 7.21 (t, J = 7.3 Hz, 1H), 7.34 (t, J = 7.8 Hz, 1H), 7.43–7.45 (m, 3H), 7.66 (t, J = 7.8 Hz, 2H), 7.74 (t, J = 8.1 Hz, 1H), 8.03 (d, J = 7.8 Hz, 1H), 12.10 (s, 1H), 12.66 (s, 1H), 16.48 (s, 1H); ^{13}C NMR (125.7 MHz, DMSO-d_6) δ 97.29, 114.89, 116.71, 121.49, 123.41, 124.76, 125.58, 129.92, 134.94, 137.51, 139.42, 163.51, 169.75, 173.06.

5.1.4. *N*-Phenyl 4-hydroxy-1-methyl-2-quinolone-3-carboxamide (6)

A mixture of **5** (180 mg, 0.64 mmol), Cs_2CO_3 (651 mg, 2 mmol) and Me_2SO_4 (253 mg, 2 mmol) in DMF (5 mL) under Ar was heated at 120 °C for 48 h. After cooling to rt, the reaction mixture was diluted with water (50 mL). The resulting precipitate was collected by filtration and dried to give **6** as a white solid (118 mg, 63%). Mp 194–196 °C; Lit. Mp 196–198 °C[34,35]; ^{1}H NMR (500 MHz, DMSO-d_6) δ 3.70 (s, 3H), 7.21 (t, J = 7.5 Hz, 1H), 7.42 (t, J = 8.0 Hz, 2H), 7.44 (d, J = 7.6 Hz, 1H), 7.68 (d, J = 7.7 Hz, 2H), 7.70 (t, J = 7.9 Hz, 1H), 7.86 (t, J = 7.8 Hz, 1H), 8.15 (d, J = 7.6 Hz, 1H), 12.69 (s, 1H), 16.60 (s, 1H); ^{1}H NMR (500 MHz, $CDCl_3$) δ 3.74 (s, 3H), 7.17 (t, J = 7.4 Hz, 1H), 7.34 (t, J = 7.5 Hz, 1H), 7.37–7.42 (m, 3H), 7.69 (d, J = 7.9 Hz, 2H), 7.72 (t, J = 8.3 Hz, 1H), 8.26 (d, J = 8.3 Hz, 1H), 12.52 (s, 1H), 16.75 (s, 1H); ^{13}C NMR (125.7 MHz, $CDCl_3$) δ 29.34, 97.18, 114.31, 116.25, 121.28, 122.63, 124.83, 125.63, 129.02, 134.00, 137.20, 139.88, 162.84, 169.38, 172.24.

5.1.5. *N*-(4-Methoxyphenyl) 4-hydroxy-6-methoxy-2-quinolone-3-carboxamide (7)

p-Methoxyaniline (123 mg, 1 mmol) was dissolved in dimethylformamide (1 ml). Then, triethyl methanetricarboxylate (232 mg, 1 mmol) was added. The mixture was heated for six hours at 170–190 °C. The reaction was cooled to rt and treated with ethanol, filtered and washed with ethanol to yield **8** as a yellow solid (143 mg, 58%); mp 308–310 °C; ^{1}H NMR (500 MHz, DMSO-d_6) δ 3.79 (s, 3H), 3.86 (s, 3H), 7.01 (d, J = 8.9 Hz, 2H), 7.40 (br s, 3H), 7.59 (d, J = 8.9 Hz, 2H), 12.01 (s, 1H), 12.63 (s, 1H), 16.67 (s, 1H); ^{13}C NMR (125.7 MHz, DMSO-d_6) δ 55.09, 55.38, 96.39, 104.22, 114.13, 114.51, 117.33, 122.13, 123.65, 129.58, 133.11, 154.53, 156.26, 161.98, 168.39, 171.37; Anal. for $C_{18}H_{16}N_2O_5$: Calcd C, 63.52; H, 4.74; N, 8.23. Found C, 63.66; H, 5.00; N, 8.09.

5.1.6. *N*-*p*-Tolyl 4-hydroxy-6-methyl-2-quinolone-3-carboxamide (8)

p-Toluidine (107 mg, 1 mmol) was dissolved in dimethylformamide (1 ml). Then, triethyl methanetricarboxylate (232 mg, 1 mmol) was added. The mixture was heated for six hours at 170–190 °C. The reaction was cooled to rt and treated with ethanol. The precipitate was washed with chloroform to give **9** as a yellow solid (137 mg, 47%); mp 324–326 °C; ^{1}H NMR (500 MHz, DMSO-d_6) δ 2.33 (s, 3H), 2.42 (s, 3H), 7.24 (d, J = 8.1 Hz, 2H), 7.36 (d, J = 8.1 Hz, 1H), 7.5–7.6 (m, 3H), 7.82 (s, 1H), 11.86 (s, 1H), 12.59 (s, 1H), 16.48 (s, 1H); ^{13}C NMR (125.7 MHz, DMSO-d_6) δ 20.14, 96.27, 113.89, 115.64, 120.50, 122.90, 129.22, 131.60, 133.72, 134.07, 135.12, 136.52, 162.38, 168.65, 171.87. Anal. for $C_{18}H_{16}N_2O_3$: Calcd C, 70.12; H, 5.23; N, 9.09. Found C, 70.44; H, 5.24; N, 9.00.

5.1.7. *N*-(4-Fluorophenyl) 6-fluoro-4-hydroxy-2-quinolone-3-carboxamide (9)

4-Fluoroaniline (111 mg, 1 mmol) and triethyl methanetricarboxylate (232 mg, 1 mmol) were mixed and heated for six hours at 170–190 °C. The reaction was cooled to rt and treated with acetonitrile, filtered and washed with acetonitrile to afford **10** as a yellow solid (114 mg, 29%); mp 334–336 °C; ^{1}H NMR (500 MHz, DMSO-d_6) δ 7.27 (t, J = 8.5 Hz, 2 H), 7.46–7.51 (m, 1H), 7.62–7.76 (m, 4H), 12.18 (s, 1H), 12.60 (s,1H), 16.43 (s,1H); ^{13}C NMR (125.7 MHz, DMSO-d_6) δ 97.03, 108.69 (d, $^2J_{CF}$ = 24.0 Hz), 114.85 (d, $^4J_{CF}$ = 8.6 Hz), 115.82 (d, $^2J_{CF}$ = 24.2 Hz), 115.82 (d, $^2J_{CF}$ = 24.2 Hz), 118.36 (d, $^3J_{CF}$ = 8.2 Hz), 122.71 (d, $^2J_{CF}$ = 25 Hz), 122.86 (d, $^3J_{CF}$ = 8.2 Hz), 122.89 (d, $^3J_{CF}$ = 8.2 Hz), 132.97 ($^4J_{CF}$ = 3 Hz), 135.46 ($^4J_{CF}$ <2 Hz), 157.37(d, $^1J_{CF}$ = 240.4 Hz), 159.0 (d, $^1J_{CF}$ = 241.8 Hz), 162.45, 168.69, 171.39 (d, $^4J_{CF}$ = 5.0 Hz). Anal. for $C_{16}H_{10}F_2N_2O_3$: Calcd C, 60.76; H, 3.19; N, 8.86. Found C, 61.00; H, 3.28; N, 8.79.

5.1.8. *N*-(2-Fluorophenyl) 8-fluoro-4-hydroxy-2-quinolone-3-carboxamide (10)

2-Fluoroaniline (111 mg, 1 mmol) and triethyl methanetricarboxylate (232 mg, 1 mmol) were mixed and heated for six hours at 170–190 °C. The reaction was cooled to rt and treated with ethanol, filtered and washed with chloroform to afford **11** as a yellow solid (20.3 mg, 10%); mp 288–290 °C; ^{1}H NMR (500 MHz, DMSO-d_6) δ 7.21–7.46 (m, 4H), 7.68 (t, J = 8.5 Hz,1H), 7.87 (d, J = 8.1 Hz, 1H), 8.30 (t, J = 7.26 Hz,1H), 12.24 (s, 1H), 12.86 (s, 1H), 16.33 (s, 1H); ^{13}C NMR (125.7 MHz, DMSO-d_6) δ 97.66, 115.66 (d, $^2J_{CF}$ = 18.7 Hz), 116.44 (d, $^3J_{CF}$ = 3.8 Hz), 119.44 (d, $^2J_{CF}$ = 16.8 Hz), 120.14 (d, $^4J_{CF}$ = 3.8 Hz), 122.78 ($^3J_{CF}$ < 2 Hz), 122.85 (d, $^3J_{CF}$ = 6.9 Hz), 125.07 (d, $^4J_{CF}$ = 3.4 Hz), 125.20 (d, $^2J_{CF}$ = 10.6 Hz), 125.96 (d, $^3J_{CF}$ = 7.7 Hz), 127.95 (d, $^2J_{CF}$ = 14.8 Hz), 149.27 (d, $^1J_{CF}$ = 247.1 Hz), 153.01 (d, $^1J_{CF}$ = 244.7 Hz), 162.97, 169.29, 172.14 (d, $^4J_{CF}$ = 3.4 Hz). Anal. for $C_{16}H_{10}F_2N_2O_3$: Calcd C, 60.76; H, 3.19; N, 8.86. Found C, 60.92; H, 3.39; N, 8.64.

5.1.9. *N*-(3-Fluorophenyl) 7-fluoro-4-hydroxy-2-quinolone-3-carboxamide (11)

3-Fluoroaniline (111 mg, 1 mmol) and triethyl methanetricarboxylate (232 mg, 1 mmol) were mixed and heated for six hours at 170–190 °C. The reaction was cooled to rt and treated with ethanol, filtered and washed with ethanol to yield **12** as a yellow solid (123 mg, 39%); mp 329–331 °C; ^{1}H NMR (500 MHz, DMSO-d_6) δ 7.05 (t, J = 8.1 Hz, 1H), 7.15 (d, J = 9.8 Hz, 1H), 7.22 (t, J = 8.5 Hz, 1H), 7.39 (d, J = 7.7 Hz, 1H), 7.41–7.48 (m, 1H), 7.67 (d, J = 11 Hz, 1H), 8.07 (t, J = 8.1 Hz, 1H), 12.18 (s,1H), 12.60 (s, 1H), 16.23 (s,1H); ^{13}C NMR (125.7 MHz, DMSO-d_6) δ 96.24, 102.06 (d, $^2J_{CF}$ = 25.0 Hz), 107.98 (d, $^2J_{CF}$ = 25.4 Hz), 111.37, 111.66 (d, $^2J_{CF}$ = 21.3 Hz), 111.66 (d, $^2J_{CF}$ = 23.4 Hz), 116.87 ($^4J_{CF}$ = 2.4 Hz), 127.66 (d, $^3J_{CF}$ = 11.9 Hz), 131.03 (d, $^3J_{CF}$ = 10.2 Hz), 138.54 (d, $^3J_{CF}$ = 11.1 Hz), 140.79 (d, $^3J_{CF}$ = 12.5 Hz), 162.39 (d, $^1J_{CF}$ = 244.0 Hz), 163.19, 165.54 (d, $^1J_{CF}$ = 250.0 Hz), 169.36, 172.18. Anal. for $C_{16}H_{10}F_2N_2O_3$: Calcd C, 60.76; H, 3.19; N, 8.86. Found C, 61.00; H, 3.31; N, 8.88.

5.2. Computational methods

5.2.1. Preparation of protein structures

The coordinates of native PI3Kα (PDB id:2RD0),[4] mutant (H1047R) PI3Kα/wortmannin complex (PDB code:3HHM),[28] and PI3K γ/Ly294002 complex (PDB id:IE7V)[46] were retrieved from the RCSB Protein Data Bank. The homology modeling module in MOE[47] was recruited to build the missing residues of 2RD0 and 1E7V. 3HHM has the same missing regions of 2RD0. Thus, 2RD0 was used as a template to fill up the missing gaps of 3HHM applying a previously described approach.[19] First, structural alignment of 3HHM to 2RD0 was performed using DaliLite[48] module of EBI tools. Second, the homology modeling generated residues of 2RD0 were adopted for 3HHM. Third, each inserted missing sequence and its surrounding residues (within 4.5 Å of the modeled

section) were energetically minimized to decrease steric clash. Fourthly, the treated proteins were prepared using the Protein Preparation[27] wizard in the Schrödinger software suite to maximize H-bond interactions.

5.2.2. Preparation of ligand structures

Test compounds (ligands) were built based on the coordinates of wortmannin in 3HHM. The ligands were built using MAESTRO build panel and subsequently minimized by MacroModel program using the OPLS2005 force field.

5.2.3. Glide docking

Two grid files for 2RD0 and 3HHM were generated using the Glide Grid Generation protocol using the bound ligands as centroids. The scaling factor for van der Waals receptor for the non-polar atoms was calibrated to 0.8 to furnish some flexibility. All other parameters were used as defaults.

5.2.4. Induced-fit docking (IFD)

The ligand was defined as a centroid in the kinase binding cleft. Both receptor and ligand Vander Waals scaling factors were set to 0.5 to allow enough flexibility for the best docked ligand pose. Other settings were determined as default. The ligand pose with the highest XP Glide score was reported.

5.3. Biological assays

5.3.1. Cell lines and reagents

HCT116, a human colon carcinoma cell line, was established in tissue culture from a primary tumor as previously described.[25] We prepared cell lines and obtained reagents as described in Refs. 17 (Supplementary data), and 21. Immunoblot analysis antibodies, poly (ADP-ribose) polymerase (PARP),[49] AKT, and phosphorylated AKT (Ser473), were obtained from cell signaling technology.

5.3.2. Cell growth inhibition

Cell growth was evaluated by an MTT [3-(4,5-dimethylthiazol-2-yl)-2,5-diphenyltetrazolium bromide] (Sigma–Aldrich, St. Louis, MO) assay using a 96-well plate read at 570 nm absorbance on microplate reader (Biotek, Winooski, VT) using Gen5 software as fully described in Ref. 17 (Supplementary data).

5.3.3. PI3K kinase assay

The cells were washed with PBS and lysed in lysis buffer, following the procedures described in Ref. 17 (Supplementary data).

5.3.4. Immunoblot analysis

Cells were lysed in TNESV lysis buffer [50 mmol/L Tris (pH 7.5), 150 mmol/L NaCl, 1% NP40, 50 mmol/L NaF, 1 mmol/L Na_3VO_4, 25 μg/mL h-glycerophosphate, 1 mmol/L phenylmethylsulfonyl fluoride, one protease inhibitor cocktail tablet (Roche, Indianapolis, IN) per 10 mL] for 30 min on ice. The supernatants were then collected by centrifugation for 15 min. Protein was determined by the Pierce BSA method. Protein samples were dissolved in 1x sample buffer (50 mM Tris, pH6.8, 1% SDS, 10% glycerol, 0.03% bromophenol blue and 1% β-mercaptoethanol). Protein (10–50 μg) was fractionated on a 10% acrylamide denaturing gel and transferred onto a nitrocellulose membrane (Life Science, Amersham) by electroblotting. The membrane was blocked with 5% nonfat dry milk in TBST [50 mmol/L Tris (pH 7.5), 150 mmol/L NaCl, 0.05% Tween 20] for 1 h at rt or overnight at 4 °C and washed in TBST. The membrane was then incubated with primary antibodies at 1:1000 dilutions for 1 h at rt or overnight at 4 °C. After washing with TBST for 30 min, the membranes were then incubated with peroxidase-conjugated goat anti-mouse or anti-rabbit IgG (Jackson Immuno Research Laboratories, Inc) at a 1:1000 dilution for 1 h at room temperature. After further washing in TBST for 30 min, the proteins were detected by the enhanced chemiluminescence (ECL) system (Amersham).

Acknowledgments

This work was partially supported by a FIRE Grant from the University of Nebraska at Omaha. DAS acknowledges Al-Zaytoonah Private University of Jordan, and a Bukey Fellowship from the University of Nebraska Medical Center for financial support. NAS and MGB acknowledge NIH (CA72001 and CA38173) for support.

Supplementary data

Supplementary data associated with this article can be found, in the online version, at http://dx.doi.org/10.1016/j.bmc.2012.09.059.

References and notes

1. Vanhaesebroeck, B.; Waterfield, M. D. *Exp. Cell Res.* **1999**, *253*, 239.
2. Vanhaesebroeck, B.; Guillermet-Guibert, J.; Graupera, M.; Bilanges, B. *Nat. Rev. Mol. Cell Biol.* **2010**, *11*, 329.
3. Cantley, L. C. *Science* **2002**, *296*, 1655.
4. Huang, C.; Mandelker, D.; Schmidt-Kittler, O.; Samuels, Y.; Velculescu, V. E.; Kinzler, K. W.; Vogelstein, B.; Gabelli, S. B.; Amzel, L. M. *Science* **2007**, *318*, 1744.
5. Zhao, L.; Vogt, P. K. *Proc. Natl. Acad. Sci. U.S.A.* **2008**, *105*, 2652.
6. Samuels, Y.; Wang, Z.; Bardelli, A.; Silliman, N.; Ptak, J.; Szabo, S.; Yan, H.; Gazdar, A.; Powell, D.; Riggins, G.; Willson, J.; Markowitz, S.; Kinzler, K.; Vogelstein, B.; Velculescu, V. *Science* **2004**, *304*, 554.
7. Liu, P.; Cheng, H.; Roberts, T. M.; Zhao, J. J. *Nat. Rev. Drug Disc.* **2009**, *8*, 627.
8. Carson, J. D.; Van Aller, G.; Lehr, R.; Sinnamon, R. H.; Kirkpatrick, R. B.; Auger, K. R.; Dhanak, D.; Copeland, R. A.; Gontarek, R. R.; Tummino, P. J.; Luo, L. *Biochem. J.* **2008**, *409*, 519.
9. Hayakawa, M.; Kaizawa, H.; Moritomo, H.; Koizumi, T.; Ohishi, T.; Okada, M.; Ohta, M.; Tsukamoto, S.; Parker, P.; Workman, P.; Waterfield, M. *Bioorg. Med. Chem.* **2006**, *14*, 6847.
10. Hayakawa, M.; Kawaguchi, K.; Kaizawa, H.; Tomonobu, K.; Ohishi, T.; Yamano, M.; Okada, M.; Ohta, M.; Tsukamoto, S.; Raynaud, F. I.; Parker, P.; Workman, P.; Waterfield, M. D. *Bioorg. Med. Chem.* **2007**, *15*, 5837.
11. Hayakawa, M.; Kaizawa, H.; Kawaguchi, K.; Ishikawa, N.; Koizumi, T.; Ohishi, T.; Yamano, M.; Okada, M.; Ohta, M.; Tsukamoto, S.; Raynaud, F. I.; Waterfield, M. D.; Parker, P.; Workman, P. *Bioorg. Med. Chem.* **2007**, *15*, 403.
12. Hayakawa, M.; Kaizawa, H.; Moritomo, H.; Koizumi, T.; Ohishi, T.; Yamano, M.; Okada, M.; Ohta, M.; Tsukamoto, S.; Raynaud, F. I.; Workman, P.; Waterfield, M. D.; Parker, P. *Bioorg. Med. Chem. Lett.* **2007**, *17*, 2438.
13. Knight, S. D.; Adams, N. D.; Burgess, J. L.; Chaudhari, A. M.; Darcy, M. G.; Donatelli, C. A.; Luengo, J. I.; Newlander, K. A.; Parrish, C. A.; Ridgers, L. H.; Sarpong, M. A.; Schmidt, S. J.; Van Aller, G. S.; Carson, J. D.; Diamond, M. A.; Elkins, P. A.; Gardiner, C. M.; Garver, E.; Gilbert, S. A.; Gontarek, R. R.; Jackson, J. R.; Kershner, K. L.; Luo, L.; Raha, K.; Sherk, C. S.; Sung, C.; Sutton, D.; Tummino, P. J.; Wegrzyn, R. J.; Auger, K. R.; Dhanak, D. *ACS Med. Chem. Lett.* **2010**, *1*, 39.
14. Heffron, T. P.; Wei, B.; Olivero, A.; Staben, S. T.; Tsui, V.; Do, S.; Dotson, J.; Folkes, A. J.; Goldsmith, P.; Goldsmith, R.; Gunzner, J.; Lesnick, J.; Lewis, C.; Mathieu, S.; Nonomiya, J.; Shuttleworth, S.; Sutherlin, D. P.; Wan, N. C.; Wang, S.; Wiesmann, C.; Zhu, B.-Y. *J. Med. Chem.* **2011**, *54*, 7815.
15. Kong, D.; Yamori, T. *Curr. Med. Chem.* **2009**, *16*, 2839.
16. Wu, P.; Hu, Y. *Curr. Med. Chem.* **2010**, *17*, 4326.
17. Sabbah, D. A.; Brattain, M. G.; Zhong, H. *Curr. Med. Chem.* **2011**, *18*, 5528.
18. Sabbah, D. A.; Simms, N. A.; Brattain, M. G.; Vennerstrom, J. L.; Zhong, H. *Bioorg. Med. Chem. Lett.* **2012**, *22*, 876.
19. Sabbah, D. A.; Vennerstrom, J. L.; Zhong, H. *J. Chem. Inf. Model.* **2010**, *50*, 1887.
20. Kametani, T.; Kigasawa, K.; Hiiragi, M. *Yakugaku Zasshi* **1965**, *85*, 871.
21. Piechaczek, J.; Bojarska-Dahlig, H. *Acta Pol. Pharm. Drug Res.* **1966**, *23*, 7.
22. Billman, J. H.; Rendall, J. L. *J. Am. Chem. Soc.* **1944**, *66*, 540.
23. Ukrainets, I. V.; Tkach, A. A.; Sidorenko, L. V.; Gorokhova, O. V. *Chem. Heterocycl. Compd.* **2006**, *42*, 1301.
24. Shi, J.; Xiao, Z.; Ihnat, M. A.; Kamat, C.; Pandit, B.; Hu, Z.; Li, P.-K. *Bioorg. Med. Chem. Lett.* **2003**, *13*, 1187.
25. Brattain, M. G.; Levine, A. E.; Chakrabarty, S.; Yeoman, L. C.; Willson, J. K. V.; Long, B. *Cancer Metastasis Rev.* **1984**, *3*, 177.
26. Samuels, Y.; Diaz, L. A.; Schmidt-Kittler, O.; Cummins, J. M.; DeLong, L.; Cheong, I.; Rago, C.; Huso, D. L.; Lengauer, C.; Kinzler, K. W.; Vogelstein, B.; Velculescu, V. E. *Cancer Cell* **2005**, *7*, 561.
27. Protein Preparation Wizard, Maestro, MacroModel, Phase, Induced Fit, Jaguar, and Glide; Schrödinger, LLC: Portland, OR, 2009.
28. Mandelker, D.; Gabelli, S. B.; Schmidt-Kittler, O.; Zhu, J.; Cheong, I.; Huang, C.; Kinzler, K. W.; Vogelstein, B.; Amzel, L. M. *Proc. Natl. Acad. Sci. U.S.A.* **2009**, *106*, 16996.
29. Boulares, A. H.; Yakovlev, A. G.; Ivanova, V.; Stoica, B. A.; Wang, G.; Iyer, S.; Smulson, M. *J. Biol. Chem.* **1999**, *274*, 22932.

30. Germain, M.; Affar, E. B.; D'Amours, D.; Dixit, V. M.; Salvesen, G. S.; Poirier, G. G. *J. Biol. Chem.* **1999**, *274*, 28379.
31. Sherman, W.; Beard, H. S.; Farid, R. *Chem. Biol. Drug Des.* **2006**, *67*, 83.
32. Sherman, W.; Day, T.; Jacobson, M. P.; Friesner, R. A.; Farid, R. *J. Med. Chem.* **2006**, *49*, 534.
33. Zhong, H.; Tran, L. M.; Stang, J. L. *J. Mol. Graphics Modell.* **2009**, *28*, 336.
34. Friesner, R. A.; Banks, J. L.; Murphy, R. B.; Halgren, T. A.; Klicic, J. J.; Mainz, D. T.; Repasky, M. P.; Knoll, E. H.; Shelley, M.; Perry, J. K.; Shaw, D. E.; Francis, P.; Shenkin, P. S. *J. Med. Chem.* **2004**, *47*, 1739.
35. Friesner, R. A.; Murphy, R. B.; Repasky, M. P.; Frye, L. L.; Greenwood, J. R.; Halgren, T. A.; Sanschagrin, P. C.; Mainz, D. T. *J. Med. Chem.* **2006**, *49*, 6177.
36. Li, Y.; Wang, Y.; Zhang, F. J. *Mol. Model.* **2010**, *16*, 1449.
37. Richter, R.; Ulrich, H. *J. Org. Chem.* **1979**, *44*, 4877.
38. Ukrainets, I. V.; Taran, S. G.; Gorokhova, O. V.; Taran, E. A.; Jaradat, N. A.; Petukhova, I. Y. *Chem. Heterocycl. Compd.* **2000**, *36*, 166.
39. Abdel-Rahman, M. H.; Yang, Y.; Salem, M. M.; Meadows, S.; Massengill, J. B.; Li, P.-K.; Davidorf, F. H. *Exp. Eye Res.* **2010**, *91*, 837.
40. Vukanovic, J.; Passaniti, A.; Hirata, T.; Traystman, R. J.; Hartley-Asp, B.; Isaacs, J. T. *Cancer Res.* **1993**, *53*, 1833.
41. Joseph, I. B. J. K.; Vukanovic, J.; Isaacs, J. T. *Cancer Res.* **1996**, *56*, 3404.
42. Vukanovic, J.; Hartley-Asp, B.; Isaacs, J. T. *Prostate* **1995**, *26*, 235.
43. Vukanovic, J.; Isaacs, J. T. *Cancer Res.* **1995**, *55*, 1499.
44. Vukanovic, J.; Isaacs, J. T. *Cancer Res.* **1995**, *55*, 3517.
45. Borgstrom, P. Torres Filho, I. P.; Hartley-Asp, B *Anticancer Res.* **1995**, *15*, 719.
46. Walker, E. H.; Pacold, M. E.; Perisic, O.; Stephens, L.; Hawkins, P. T.; Wymann, M. P.; Williams, R. L. *Mol. Cell* **2000**, *6*, 909.
47. The Molecular Operating Environment (MOE); Chemical Computing Group Inc.: Montreal, QC, Canada, 2009.
48. Holm, L.; Park, J. *Bioinformatics* **2000**, *16*, 566.
49. Hayashi, K.; Tanaka, M.; Shimada, T.; Miwa, M.; Sugimura, T. *Biochem. Biophys. Res. Commun.* **1983**, *112*, 102.